

## High frequency blade surface temperature determination using surface mounted hotfilm gauges

**Maik Tiedemann**

Institute of Propulsion Technology  
 German Aerospace Center (DLR)  
 Göttingen, Germany

### ABSTRACT

This paper describes an attempt to determine total temperature fluctuations on the surfaces of the rotor of a transonic high pressure turbine stage. The gathered results were used to evaluate the error that these fluctuations cause in the constant temperature anemometer output signal of surface mounted hotfilms.

As the temperature variations in turbomachines occur at frequencies in the order of the blade passing frequency (usually several kHz), it is in most cases not feasible to measure the surface temperature directly. Therefore, an indirect method was developed which determines the temperature fluctuations from the results of two different hotfilm tests.

Even though the results are subject to severe errors, the method provides interesting information on the nature of the temperature fluctuations on the blade surfaces. The results show, that in the investigated case of a transonic turbine rotor, the temperature variations did not have a significant effect on the qualitative wall shear stress. However, this might be entirely different in other set-ups, particularly when measurements are performed downstream of turbomachinery rotors.

### NOMENCLATURE

a	$[(W^3 m^2 / K^3 N)^{1/3}]$	constant
A	$[m^2]$	area
$c_p$	$[J/kgK]$	specific heat
$l_1$	$[\ ]$	shape function integral of temperature profiles
L	$[m]$	length
$p_r$	$[mW]$	power random fluctuations
P	$[mW]$	power, CTA output
R	$[\Omega]$	resistance
s	$[m]$	surface length, $s=0$ at stagnation point
T	$[K]$	temperature
V	$[V]$	voltage
$\Delta T$	$[K]$	hotfilm overheat temperature
$\eta$	$[Pa s]$	dynamic viscosity
$\lambda$	$[W/m K]$	thermal conductivity
$\rho$	$[kg/m^3]$	density
$\tau_w$	$[N/m^2]$	wall shear stress

### Subscripts

0	stagnation value, zero-flow condition
1, 2	test indices, inlet/exit

eff	effective
gauge	gauge
gh	property of heated gauge
i	index of time steps
ps, ss	pressure side, suction side
W	wall

### Superscripts

$\sim$	ensemble-averaged value
—	time-averaged value

### 1. INTRODUCTION

Surface mounted hotfilm gauges operated in constant temperature mode are often utilized for the qualitative determination of wall shear stresses. The magnitude of the output signals of these gauges is a function of the overheat temperature  $\Delta T$  which is the difference between the recovery temperature of the flow and the temperature of the gauge. As the gauge temperature is kept constant by the constant temperature anemometer circuit (CTA), variations of  $\Delta T$  can only result from variations of the flow temperature. Since temperature-induced signal variations are not caused by variations in the wall shear stress, they must be considered measurement errors. According to Bellhouse & Schultz (1966), temperature changes in the order of magnitude of 0.1 K may already cause significant errors.

The flow exiting a turbomachinery blade row often shows significant total temperature variations which may affect surface hotfilm measurements on downstream blade rows. The work described here was conducted in order to investigate the influence of such temperature variations on hotfilm measurements on a transonic high pressure turbine (HPT) rotor which were part of a European research program. The actual hotfilm measurements are described in detail by Tiedemann & Kost (1999).

The total temperature variation downstream of the nozzle guide vane (NGV) of the investigated turbine stage, measured with only the NGV installed (the rotor gap was covered with a liner ring), is given in **Figure 1**. Since the NGV inlet temperature  $T_{01}$  was constant, the plotted temperature differences are solely due to temperature variations in the NGV exit flowfield. The observed redistribution of energy downstream of the adiabatic stator vane, was presumably caused by the counter-rotating vortices in its wake. (see e.g. Kurosaka et al. (1987), Eckert (1986), and Carscallen & Oosthuizen (1990)).

**Figure 1** indicates temperature variations of approximately 4 K at 0.25 axial NGV chords downstream of the NGV trailing edge, which is close to the leading edge position of the rotor. Due to the facts that 4 K are in the order of 6% to 10% of the utilized overheat temperatures, and that the temperature fluctuation may be even larger in the relative frame of reference, it seemed worthwhile to investigate the measurement error which is due to these variations.

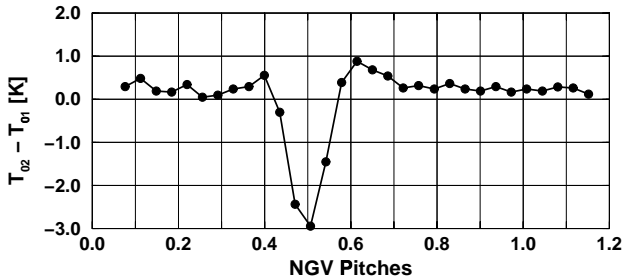


Figure 1: Total temperature profile downstream of the NGV;  $x/c_{ax,NGV} = 0.25$

The transition from the relative frame of reference to the absolute frame may cause total temperature variations downstream of turbomachinery rotors which are much higher than those observed here. Epstein et al. (1988) report total temperature fluctuations downstream of a compressor rotor of  $\pm 10$  to 20 K. Thus, a method to correct errors due to variations of hotfilm overheat temperatures would also be very useful for other applications of the surface hotfilm technique. Note, that phase shifts and phase reversals due to temperature effects may result in misleading conclusions, even in investigations where only a qualitative evaluation of the hotfilm signals is performed.

As the temperature variations in turbomachines occur at frequencies in the order of the blade passing frequency (usually several kHz), it is in most cases not feasible to measure the time-resolved surface temperature directly. This paper describes an attempt to circumvent this problem by determining the temperature fluctuations utilizing two different hotfilm tests.

## 2. EXPERIMENTAL APPARATUS

### 2.1 The “Windtunnel for Rotating Cascades” (RGG)

The experiments described in this paper were conducted in the “Windtunnel for Rotating Cascades” (RGG) of the DLR in Göttingen, which is a closed circuit, continuously running windtunnel. A four stage radial compressor (maximum pressure ratio: 6) driven by a speed-controlled 1 MW dc-motor provides a volume flow rate of up to 15.5 m<sup>3</sup>/s. All components of the facility are accurately controlled by means of a “Simatic S5” industrial control system. Possible rotor speeds are up to 10,000 RPM in both directions. The rotor is coupled to a speed-controlled 500 kW dc-motor/generator which can drive or brake the rotor in either direction.

For a choked NGV (typical for HPTs), the stage inlet Mach number is determined by the vane geometry. The static pressure downstream of the NGV throat (and thus the stage pressure ratio and the NGV exit Mach number) is coupled to the rotational speed of the main compressor. Since the Reynolds number depends mainly on the adjustable settling chamber pressure and temperature levels, Mach and Reynolds number can be varied independently within certain limits.

### 2.2 The turbine stage

The utilized turbine stage was designed by Alfa Romeo Avio

in the course of a European turbine project. It comprises a state-of-the-art, full size, transonic, aero-engine HPT. The geometry at mid-span (where this investigation was conducted) is given in **Table 1** while **Table 2** shows some of the stage operating parameters. **Figure 2** shows the stage and the positions of the hotfilm gauges (20 suction side and 14 pressure side gauges).

Table 1: Geometrical parameters of the turbine blade rows

	NGV	Rotor
Axial chord	29.86 mm	27.45 mm
Tip radius	274.00 mm	274.00 mm
Hub radius (inlet)	238.84 mm	238.84 mm
Number of blades	43	64

Table 2: Operating parameters of the turbine stage

absolute NGV exit Mach number	0.937
relative rotor exit Mach number	0.938
absolute NGV exit Reynolds number	$0.866 \cdot 10^6$
relative rotor exit Reynolds number	$0.396 \cdot 10^6$
rotor speed	[1 / min] 7894.0
stage total to total pressure ratio	2.64

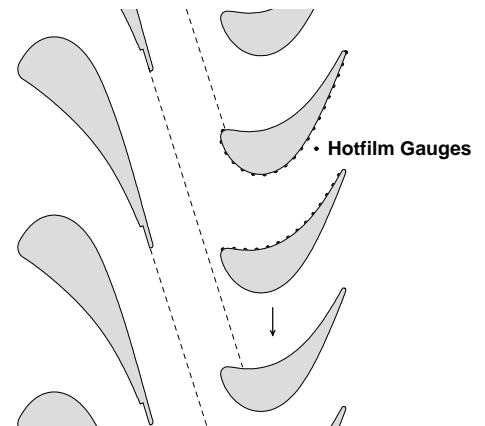


Figure 2: Stage configuration at mid-span

### 2.3 Measurement technique and data acquisition

The surface hotfilm technique is very similar to hot wire anemometry. The power required to keep the hotfilm resistance (and thereby the temperature) constant depends on the heat transfer towards the fluid which is related to the wall shear stress. The used gauge overheat temperatures of 60 K and 40 K were set by soldering fixed resistances into the adjust arm of the Wheatstone bridge. The cut-off frequency of the gauges of approximately 15-20 kHz was sufficient to resolve the first three harmonics of the vane passing frequency (5.66 kHz).

The signals from the utilized MTU hotfilm gauges (which were glued onto the rotor surfaces) were processed by two rotating CTAs. The different gauges and their respective adjust resistors were successively switched into the CTA bridge. An optoelectronic system was used to transmit the CTA output signals to the stationary frame of reference. The CTAs and the transmission system were developed by the University of Limerick (see Davies et al. (1997) for details). A shaft encoder triggers the PC-based A/D converter. Afterwards, exactly one sample is taken for each of the 1024 pulses the encoder delivers per revolution. This technique guarantees that the samples are taken at the same NGV/rotor position in every revolution (see Tiedemann (1998) for details on the data acquisition system).

### 3. TEMPERATURE DETERMINATION METHOD

Hotfilm gauges can be used as resistance thermometers when operated in constant current mode. This technique is, however, limited to very low temperature fluctuation frequencies (app. 400 Hz). In this section a method is described which allows for temperature measurements up to several kHz. The basic idea of this technique is to conduct two tests under identical flow conditions but at different hotfilm overheat temperatures.

Prior to the actual data evaluation, the sampled CTA signals were corrected for offset, phase shift, and attenuation errors. According to Bellhouse and Schultz (1966), the voltage drop over the gauge  $V$  is related to the wall shear stress  $\tau_W$  by:

$$\frac{V^2}{R} - \frac{V_0^2}{R_0} = P - P_0 = a \tau_W^{\frac{1}{3}} (T_{gh} - T_W) \quad (1)$$

$V$  is the voltage drop over the actual gauge, which can be computed from the CTA output signal and the known resistances in the CTA bridge.  $P_0$  is the dissipated power at zero-flow. Since the surface temperatures at zero-flow and during the actual test differed significantly, calibration curves for  $P_0$  vs.  $\Delta T = (T_{gh} - T_W)$  had to be determined.

$T_W$  is the fluid temperature that would be attained at the wall, without the (heated) gauge installed. This temperature and the wall shear stress  $\tau_W$  are entirely independent of the hotfilm temperature  $T_{gh}$ , but are solely determined by the flow parameters

Two hotfilm tests, carried out under identical flow conditions but at different gauge temperatures, lead to a set of two equations:

$$P_{1,i} - P_{01} = (a_1 \tau_W^{\frac{1}{3}})_i (T_{gh,1} - T_{W,i}); \quad i = 0 \dots 1023 \quad (2)$$

$$P_{2,i} - P_{02} = (a_2 \tau_W^{\frac{1}{3}})_i (T_{gh,2} - T_{W,i}); \quad i = 0 \dots 1023 \quad (3)$$

where the indices 1 and 2 refer to the two different tests and the subscript "i" denotes the circumferential measurement positions (NGV/rotor phase angle). The gauge hot temperatures  $T_{gh}$  are set by means of fixed resistances, and the values on the left-hand side are measurement results. Thus, the constants  $a_1$  and  $a_2$ , the wall shear stress, and the wall temperature are the remaining unknowns in these equations.

The flow parameters are only identical in the two tests if both, the unsteady and the steady flowfields, are reproducible. The stochastic components of the two signals are definitely different. However, the periodically unsteady ensemble-averaged data traces are reproducible in a turbomachinery environment and can therefore be used in the above equations.

Considering that the gauge heats only a very small portion of the flow, it is a reasonable assumption, that temperature dependant flow parameters such as density and viscosity are identical in the two test cases, even though the gauge temperatures are different. Thus, in the constant "a", given by (Hauelsen 1996):

$$a = \left( \frac{\rho c_p l_1 \lambda^2 A_{\text{eff}}^3}{\eta L_{\text{eff}}} \right)^{\frac{1}{3}} \quad (4)$$

only the effective gauge area  $A_{\text{eff}}$  and the effective gauge length  $L_{\text{eff}}$  depend on the overheat temperature. The mean values of the other parameters remain constant as long as the flow parameters remain unchanged. Note, that the effectively heated area may be significantly larger than the geometrical gauge dimensions.

An infrared camera was used to take thermal images of a sample gauge at those overheat temperatures that were applied during the actual tests. These images showed, that the effective width is almost identical in both cases, i.e. it cancels out when the ratio of the two constants in equations 2 and 3 is formed:

$$\frac{a_2}{a_1} = \left( \left( \frac{A_{\text{eff},2}}{A_{\text{eff},1}} \right)^3 \frac{L_{\text{eff},1}}{L_{\text{eff},2}} \right)^{\frac{1}{3}} = \left( \frac{L_{\text{eff},2}}{L_{\text{eff},1}} \right)^{\frac{2}{3}} \quad (5)$$

From the above-mentioned thermal images of the gauges, the ratio of the effective lengths  $L_{\text{eff},2}/L_{\text{eff},1}$  was determined to be 0.84. Therefore, the ratio  $a_2/a_1$  for these particular sets of tests was approximately 0.89.

Using this ratio and rearranging equations 2 and 3, the terms  $(a_1 \tau_W^{\frac{1}{3}})_i$ ,  $(a_2 \tau_W^{\frac{1}{3}})_i$ , and the wall temperature yield:

$$(a_1 \tau_W^{\frac{1}{3}})_i = \frac{\tilde{P}_{1,i} - P_{01}}{T_{gh,1} - T_{W,i}}; \quad i = 0 \dots 1023 \quad (6)$$

$$(a_2 \tau_W^{\frac{1}{3}})_i = \frac{a_2}{a_1} \frac{\tilde{P}_{1,i} - P_{01}}{T_{gh,1} - T_{W,i}}; \quad i = 0 \dots 1023 \quad (7)$$

$$T_{W,i} = \frac{T_{gh,1} (\tilde{P}_{2,i} - P_{02}) - \frac{a_2}{a_1} T_{gh,2} (\tilde{P}_{1,i} - P_{01})}{\tilde{P}_{2,i} - P_{02} - \frac{a_2}{a_1} (\tilde{P}_{1,i} - P_{01})}; \quad i = 0 \dots 1023 \quad (8)$$

The trace of  $T_{W,i}$  is the time-resolved wall temperature distribution that would be attained at a particular gauge position if the gauge were not installed. Its frequency resolution is similar to that of the ensemble-averaged hotfilm signals  $\tilde{P}_{1,i}$  and  $\tilde{P}_{2,i}$ .

The time-mean value of  $T_W$  can now be used to correct the CTA output values of a certain gauge, as if they were all taken at the same overheat temperature  $\Delta T$ . Due to the fact that the term  $(a_1 \tau_W^{1/3})_i$  is independent of  $\Delta T$ , this correction can be performed by replacing  $T_{W,i}$  with  $\overline{T_W}$  in equation 2, thus:

$$\tilde{P}_{1,i} - P_{01} = (a_1 \tau_W^{\frac{1}{3}})_i (T_{gh,1} - \overline{T_W}); \quad i = 0 \dots 1023 \quad (9)$$

Note, that this correction method is only valid if  $P$  and  $\Delta T$  are linearly dependant. However, this requirement is often fulfilled.

For the determination of a signal that is a measure of the wall shear stress, the signal trace of  $(a_1 \tau_W^{1/3})_i$  is much more appropriate than that of the corrected  $\tilde{P} - P_0$  because it is independent of  $\Delta T$ . However, the correction will be performed in the next section to enable the determination of the effect of temperature fluctuations on hotfilm signals, by comparing the results with and without temperature correction.

Theoretically, the time-mean value of  $T_W$  must equal the time-mean wall temperature as measured via the hotfilm resistances (constant current mode measurements). Thus, the comparison of these two values provides a good means to check the validity of the method. It should be noted that this method is valid only if the equation it is based upon (equation 1) is valid. The following list comprises some of the assumptions that were made during the derivation of this equation (Hauelsen 1996):

- steady, incompressible flow
- layered flow in the proximity of the wall
- temperature boundary layer thickness is small compared to the boundary layer thickness
- no pressure gradient in flow direction

Some of these assumptions are certainly not valid for the unsteady, compressible, and over extended surface portions accelerated flow on the turbine rotor under investigation. Nevertheless, in order to gather informations on the impact of temperature effects on the data, the developed method was applied to the sampled CTA output signals. In the following sections this method will be referred to as the "twin test method".

#### 4. RESULTS AND DISCUSSION

In this section some examples of unsteady temperature traces, which were determined by means of the method described in the preceding section, are presented and discussed.

The bottom plot in **Figure 3** shows a comparison of time-averaged wall temperature measurements on the pressure side of the blade. The dashed line was measured by utilizing the hotfilm gauges as resistance thermometers. Even though this method is known to be rather inaccurate, it is the only reference measurement that could be performed during this investigation. Considering the fact that the measured temperature in the leading edge region was close to the theoretical stagnation point value of approximately 272 K, it appears, however, sufficiently accurate to serve as a reference for the twin test method. The solid line in the bottom plot represents the time-averaged wall temperatures as determined by means of the twin test method. The plot shows some quite significant differences between the two curves. On the other hand, the temperatures which were determined by means of the new method seem to be of the correct order of magnitude, which is an indication for the validity of the method. In the trailing edge region, the differences between the twin test method values and the resistance mode results differ by the same order of magnitude from the theoretical wall temperature value of 267 K (computed by assuming fully turbulent flow and a recovery factor of  $\sqrt[3]{Pr}$ , Prandtl number  $Pr = 0.71$ ). All in all, the time-averaged values of the two temperature measurements were in reasonably good agreement in this case.

The center plot in **Figure 3** shows the time-averaged hotfilm power dissipation towards the fluid, normalized by the zero-flow power dissipation  $P_0$ . The dashed line shows the original (uncorrected) plot, while the solid line represents the same data, corrected according to equation 9. The figure clearly shows that the influence of the temperature effect on the time-average of the data

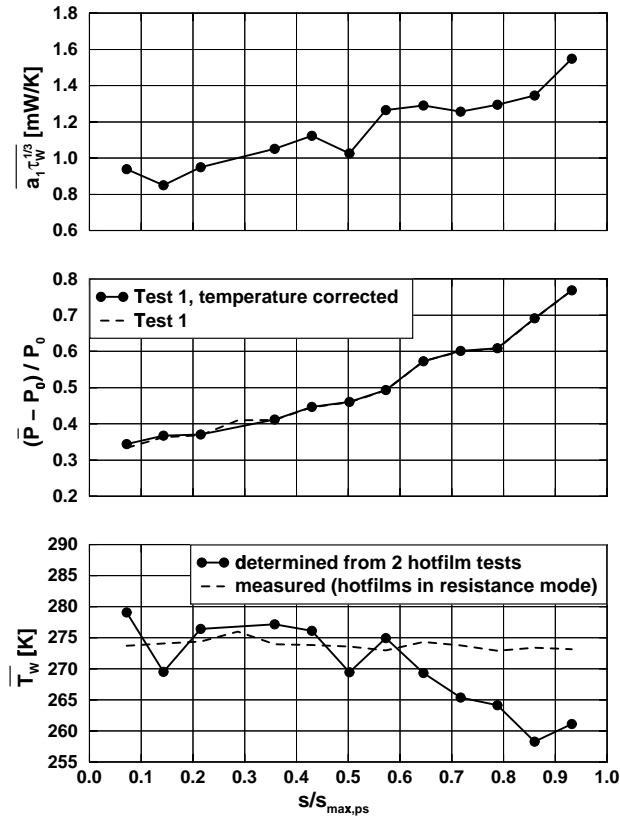


Figure 3: Time-averaged hotfilm and temperature data; pressure side

was negligible. The time-averaged values of  $(a_1 \tau_W^{1/3})$ , given in the top plot of **Figure 3**, indicate a similar boundary layer behavior as the  $(\bar{P} - P_0)/P_0$  values. The two curves differ only in the regions around  $s/s_{max,ps} = 0.14$  and  $0.5$ . These are exactly those regions, where the wall temperature distribution deviates most from a smooth curve. Taking into account that the time-averaged temperature distribution along the wall was most certainly very smooth (due to heat conduction), these extreme values indicate errors in the determination of the wall temperature level. Thus, the changes in  $(a_1 \tau_W^{1/3})$  were more likely induced by errors in  $\bar{T}_W$  than by changes of the wall shear stress. The possible causes of these errors will be discussed below.

**Figure 4** shows the time traces of the first active gauge on the pressure side ( $s/s_{max,ps} = 0.07$ ). The Signals 1 and 2 were measured at overheat temperatures of  $\Delta T = 60K$  and  $\Delta T = 40K$ , respectively. The shape of the temperature corrected trace in the second plot is similar to that of the two original traces, given in that same plot. Some features are, however, more pronounced in the corrected signal. This is particularly true for the secondary maxima which appear between the large local maxima. Thus, the corrected signal contains the same general informations as the original one, but the two signals differ in some secondary features. The reason for this amplification of certain features is presumably the difference in the resolution of the two original signals. It seems that features which are only present in one of the traces are artificially amplified in the twin test method.

The information provided by the traces of  $(a_1 \tau_W^{1/3})$  is very similar to that of the uncorrected  $(\bar{P} - P_0)/P_0$  traces. This means, that, even though the wall temperature (third plot of **Figure 4**) showed significant fluctuations of approximately  $\pm 8 K$ , it

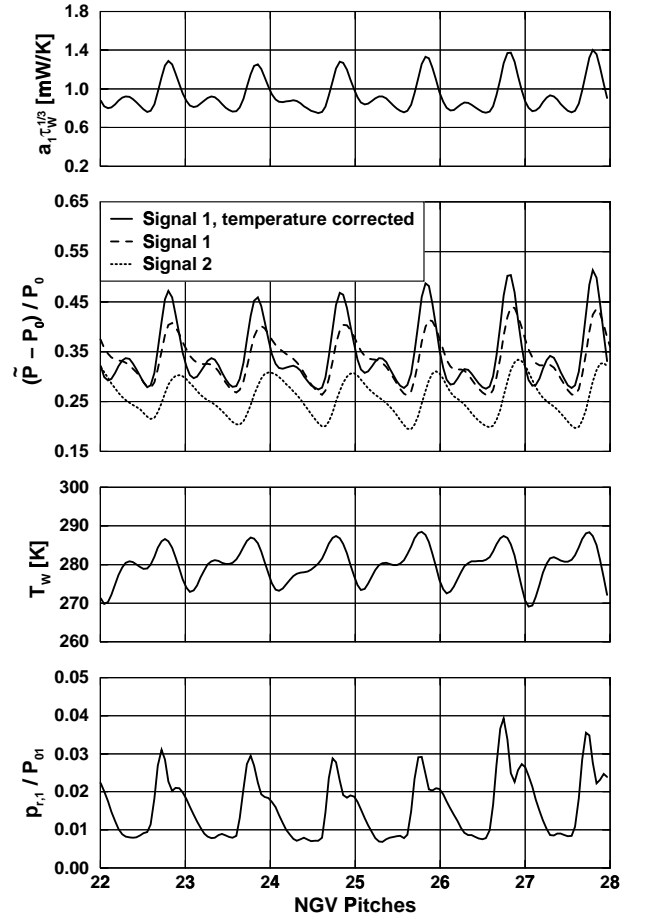


Figure 4: Time-resolved hotfilm and temperature data; pressure side,  $s/s_{max,ps} = 0.07$

did not change the general qualitative pattern of the hotfilm signal traces.

The temperature variations downstream of the NGV decay with increasing distance to the trailing edge. For this reason, the effects of NGV exit temperature fluctuations on the rotor instrumentation are strongest in the rotor leading edge region, which was confirmed by the data of the remaining gauges (not presented). Thus, in this case the temperature fluctuations had only a minor influence on the time-resolved hotfilm signals which were obtained on the rotor pressure surface. Note, that the temperature trace has the same resolution and therefore the same frequency range as the ensemble-averaged hotfilm signal. The random fluctuations are plotted in the bottom plot of **Figure 4** to indicate the location of the wakes (maxima of  $p_r$ ).

The time-averaged values plotted in **Figure 3** for the pressure side of the rotor, are given in **Figure 5** for the suction side. Similar to the pressure side, the normalized, time-averaged hotfilm power dissipation  $(\bar{P} - P_0)/P_0$  did not significantly change when the temperature correction was applied. This implies that the influence of the unsteady temperature field on the time-mean values was negligible.

The two wall temperature distributions given in the bottom plot of **Figure 5**, show differences of up to 30 K between the measured values and the temperatures determined by means of the twin test method. The primary effect of this error is that the distribution of  $(a_1 \tau_W^{1/3})$ , shown in the top plot, differs from the distribution of the hotfilm signal in the center plot. This effect is caused by the high temperature level that pretended lower overheat temperatures  $\Delta T$ , which in turn led to increased values of  $(a_1 \tau_W^{1/3})$ . Since the obviously elevated temperature levels appeared mainly in the forward region of the blade, the  $(a_1 \tau_W^{1/3})$  distribution in this region was also elevated. Thus, it appears very likely that the differences between the two distributions were caused by the er-

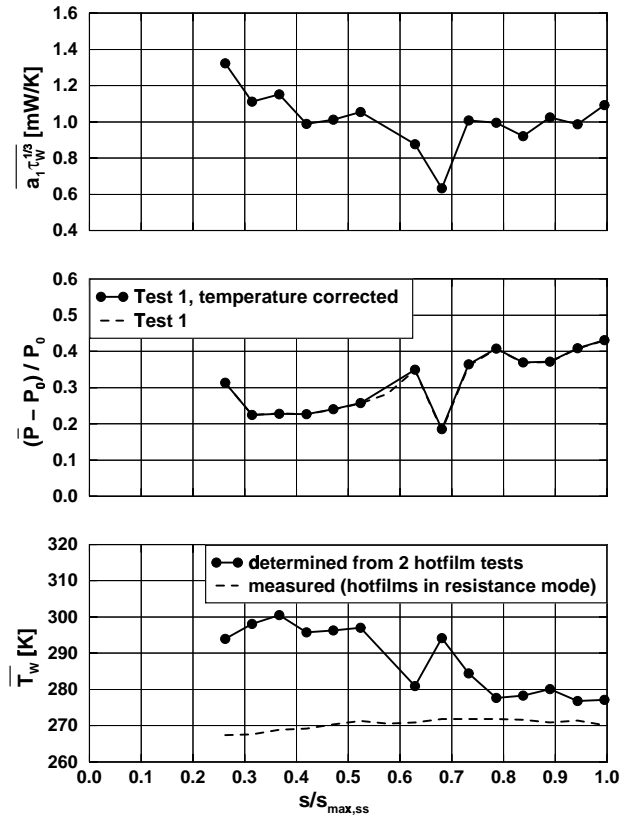


Figure 5: Time-averaged hotfilm and temperature data; suction side

ror in the wall temperature determination. The average wall temperature values are strongly affected by the accuracy of the zero-flow hotfilm power dissipation  $P_0$ . If the accuracy of the  $P_{0,i}$  values in equations 2 and 3 is insufficient, the resulting error in the temperature level can become unacceptable. It seems, that in this case the accuracy of the  $P_{0,i}$  values was not sufficient for the application of the twin test method.

**Figure 6** shows the time-resolved signals of the first active gauge ( $s/s_{max,ss} = 0.262$ ) on the suction surface of the rotor blade. The time traces of the hotfilm and the  $(a_1 \tau_W^{1/3})$  signals indicate a similarly small effect of the unsteady temperature distribution on the hotfilm signals as on the pressure side. Note that even though the level of the wall temperature was entirely wrong, the temperature fluctuations remained within a reasonable range. Apparently, the unsteady results of the twin test method seem to be valid, even when the time-mean values are not correct.

The reasons for the errors in the wall temperature, determined by means of the twin test method, are assumed to be three-fold. First of all, the temperature level reacts very sensitively to inaccuracies in the determination of the zero-flow power dissipation  $P_{0,i}$ . Secondly, the resolution (cut-off frequency) of the two signals must be absolutely identical to ascertain that both signals contain the same features. If this is not the case, certain features which are contained in only one of the signals are artificially amplified. Therefore, the twin test method requires an equipment which enables the accurate determination of  $P_{0,i}$  and which is capable of operating with the same frequency response set-up at different overhear temperatures, i.e. the CTA must be stable over large ranges of  $\Delta T$ . The rotating equipment used in this investigation, does not fulfill either one of these requirements over the

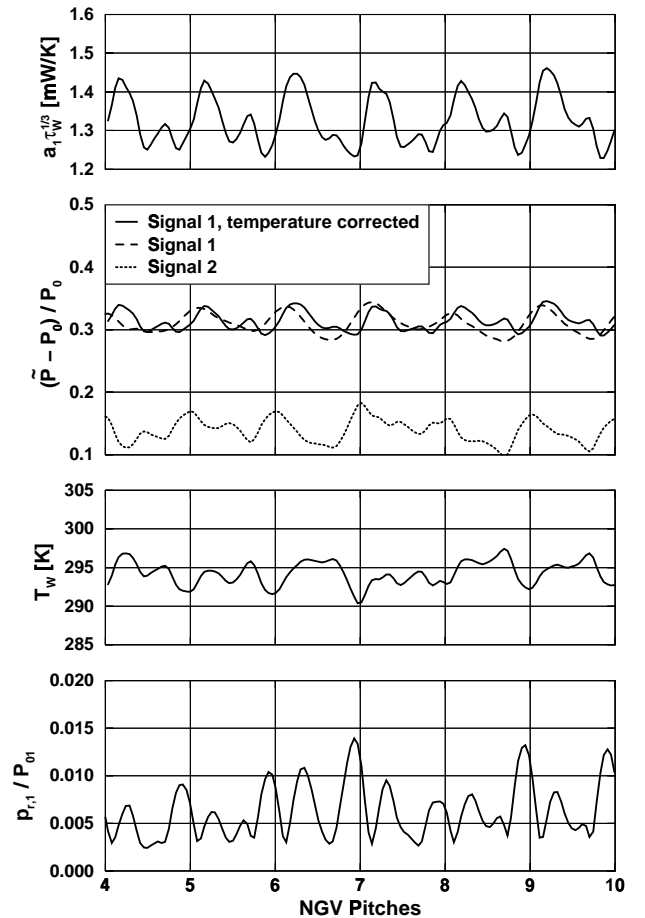


Figure 6: Time-resolved hotfilm and temperature data; suction side,  $s/s_{max,ss} = 0.26$

entire operating ranges of all test cases. Due to the prototype nature of the CTAs and the challenging conditions under which measurements in the rotating frame of reference are performed, certain features of the measuring equipment were far away from being optimally suited for the particular requirements of the twin test method. Setting the overheat temperature by means of fixed resistances, the accuracy of the gauge resistance determination, and the operation close to the frequency response limit of the system, are only some of these features. Therefore, the performance of the relatively small CTA boards is certainly not as good as that of the much more complex and specialized (and bulky) stationary equipment available. This gives rise to the hope that the method might perform better when more sophisticated (stationary) equipment is used.

The third possible reason for the errors in the computed wall temperature are the assumptions that were made during the derivation of the governing equations of the twin test method. As mentioned above, some of these assumptions are certainly not valid in the investigated case. Despite these draw-backs, the method provided useful information and shows some potential for improvements when utilizing more sophisticated equipment.

## 5. CONCLUSIONS

A method for the determination of time-resolved temperature signals based on two different hotfilm measurements was presented. The method was applied to surface mounted hotfilm measurements in a transonic high pressure turbine stage. The results were used to investigate the effects of temperature fluctuations on hotfilm signals and the possible measurement errors these fluctuations may cause. Even though the temperature correction by means of the new method is obviously subject to errors, the method proved very useful for the determination of qualitative effects of temperature fluctuations on hotfilm results.

The assumed reasons for the errors in the wall temperature determined by means of the twin test method are: inaccuracies in the determination of the zero-flow power dissipation  $P_{0,i}$ , differences in the resolution (cut-off frequency) of the two signals, and the fact that some of the assumptions that were made during the derivation of the governing equations of the method are not valid in the investigated case. Apparently, the twin test method requires an equipment which enables the accurate determination of  $P_{0,i}$  and which is capable of stable operation over large ranges of  $\Delta T$ .

It turned out that the qualitative signals in this particular investigation were not significantly affected by the determined temperature variations. However, it should be kept in mind that temperature variations downstream of rotors or second or higher stage stators may be significantly larger than those downstream of this first stage stator. Thus, the effect of these variations on the CTA signals may not be negligible there. Fortunately, as the stationary equipment used for hotfilm gauges on stator vanes is much more appropriate for the application of the twin test method, the correction of temperature effects downstream of rotors might be much more successful.

## ACKNOWLEDGMENTS

The author gratefully acknowledges the technical support by E. Schüpferling, A. Tappe, and A. Uhl during the tests and the data acquisition.

## REFERENCES

- Bellhouse, B.J., Schultz, D.L., 1966, "Determination of mean and dynamic skin friction, separation and transition in low-speed flow with a thin-film heated element" *Journal of Fluid Mechanics*, Vol. 24, Part 2, pp 379-400.
- Carscallen, W.E., Oosthuizen, P.H., 1990, "The effect of secondary flow on the redistribution of the total temperature field downstream of a stationary turbine cascade" *AGARD-CP-469*, pp 27-1 - 27-18.
- Eckert, E.R.G., 1986, "Energy separation in fluid streams" *Int. comm. heat mass transfer*, Vol 13, pp 127-143, Pergamon Press USA.
- Epstein, A.H., Gertz, J.B., Owen, P.R., Giles, M.B., 1988, "Vortex shedding in high-speed compressor blade wakes" *AIAA Journal of Propulsion*, Vol. 4, No.3, pp 236-244.
- Haueisen, V., 1996, "Untersuchungen des Grenzschichtumschlags am Kreiszyylinder bei unterschiedlichen stationären und instationären Zuströmbedingungen" *Doctoral dissertation TH Darmstadt*.
- Kurosaka, M., Gerz, J.B., Graham, J.E., Goodman, J.R., Sundaram, P., Riner, W.C., Kuroda, H., Hankey, W., 1987 "Energy separation in a vortex street" *Journal of Fluid Mechanics*, Vol. 178, pp 1-29.
- Tiedemann, M., 1998, "Investigation of the unsteady boundary layer transition in a transonic high pressure turbine stage" *Doctoral dissertation, TU Darmstadt; also available as DLR-FB 98-30*.
- Tiedemann, M., Kost, F., 1999, "Unsteady boundary layer transition on a high pressure turbine rotor blade" *ASME Paper 99-GT-194*.